IAC-20-A7.2.4

Overview and status of EXCLAIM, the experiment for cryogenic large-aperture intensity mapping

Giuseppe Cataldo[a*], Emily M. Barrentine[a], Nicholas G. Bellis[a], Thomas R. Essinger-Hileman[a], Luke N. Lowe[a], Philip D. Mauskopf[b],Anthony R. Pullen[c], Eric R. Switzer[a]

[a]*NASA Goddard Space Flight Center, 8800 Greenbelt Road, Greenbelt, MD 20771, U.S.A.*

[b]*School of Earth and Space Exploration, Arizona State University, Tempe, AZ 85287, U.S.A.*

[c]*Center for Cosmology and Particle Physics, New York University, 726 Broadway, New York, NY 10003, U.S.A.*

* Corresponding Author: Giuseppe.Cataldo@NASA.gov

Abstract

The EXperiment for Cryogenic Large-Aperture Intensity Mapping (EXCLAIM) is a balloon-borne far-infrared telescope that will survey star formation history over cosmological time scales to improve our understanding of why the star formation rate declined at redshift $z < 2$, despite continued clustering of dark matter. Specifically, EXCLAIM will map the emission of redshifted carbon monoxide and singly ionized carbon lines in windows over a redshift range $0 < z < 3.5$, following an innovative approach known as intensity mapping. Intensity mapping measures the statistics of brightness fluctuations of cumulative line emissions, as opposed to detecting individual galaxies, thus enabling a blind, complete census of the emitting gas. To detect this emission unambiguously, EXCLAIM will cross-correlate with a rich spectroscopic galaxy catalog. The EXCLAIM mission will use a cryogenic design to cool the telescope optics to approximately 1.7 K. The telescope will feature a 90-cm primary mirror to probe spatial scales on the sky from the linear regime up to shot-noise-dominated scales. The telescope optical elements will couple to six μ-Spec spectrometer modules, operating over a 420–540-GHz frequency band with a spectral resolution of 512 and featuring Microwave Kinetic Inductance Detectors (MKIDs). In the baseline design, the detectors will be read out with a Radio Frequency System-on-Chip (RFSoC). The cryogenic telescope and the sensitive detectors will allow EXCLAIM to reach high sensitivity in spectral windows of low emission in the upper atmosphere. Here, an overview of the mission design and development status since the start of the EXCLAIM project in early 2019 is presented.

Keywords: Intensity mapping, star formation, balloon telescope, infrared spectrometer.

1. Introduction

Observations of our universe over cosmological time [1] indicate an increase in the rate of star formation from the period of cosmological reionization up to redshifts $z \approx 2$. Following this peak, the star formation rate is thought to fall by a factor of 20, all while dark matter continues to cluster 100-fold [2]. To gain a better understanding of the aggregate evolution of galaxies in this cosmological context, new measurements are needed of the typical abundance, excitation and evolution of the molecular gas that forms and is influenced by stars. The EXperiment for Cryogenic Large-Aperture Intensity Mapping (EXCLAIM) is a high-altitude balloon-borne telescope that will address this scientific need by mapping the submillimeter emission of redshifted carbon monoxide (CO) and [CII] lines in windows varying over $0 < z < 3.5$.

Rather than detecting individual galaxies, EXCLAIM will measure the statistics of brightness fluctuations of redshifted, cumulative line emission, an approach known as intensity mapping (IM). IM is sensitive to the integral of the luminosity function in cosmologically large volumes and to tracers of several environments in the interstellar medium (ISM).

In its baseline survey, EXCLAIM will map emission over a 420–540 GHz frequency band with resolving power $R = 512$ on a 408 deg^2 region of the sky that overlaps with the Baryon Oscillation Spectroscopic Survey (BOSS) [3] and a 90 deg^2 region in the plane of the Milky Way. Even though the optimal band for BOSS cross-correlation is 420–600 GHz, in EXCLAIM this is truncated at 540 GHz to avoid bright ortho-water emission in the upper atmosphere at 557 GHz. The broad survey area provides access to linear density fluctuations, which are easier to interpret than clustering within halos. EXCLAIM's primary extragalactic science is done by cross-correlation, to facilitate unambiguous detection of redshifted emission in the presence of foregrounds.

EXCLAIM's scientific goals can be summarized as

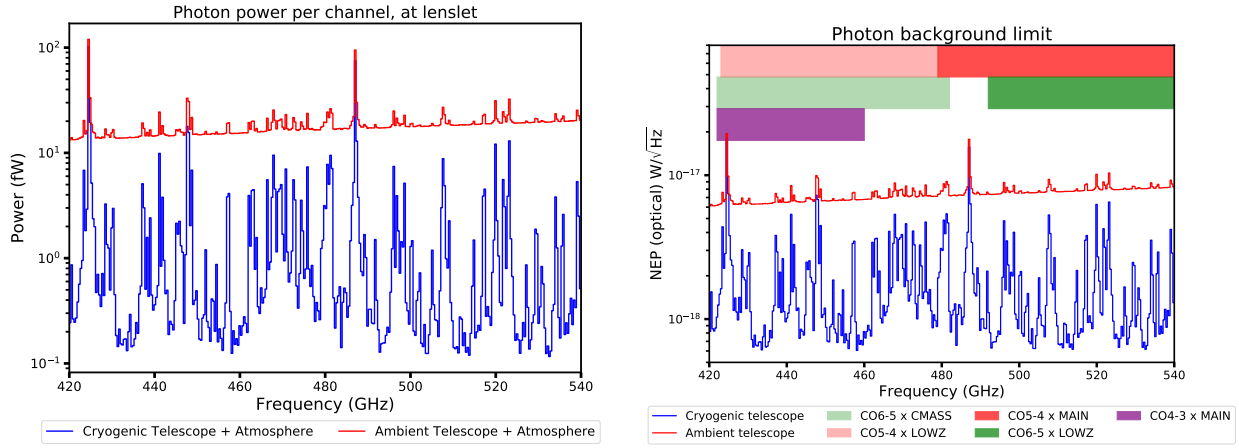

Fig. 1: Photon loading (left) and background-limited optical NEP (right), both measured at the spectrometer lenslet input and assuming an overall telescope coupling efficiency of 60%. The background limit includes optically-excited quasiparticles and assumes 30% spectrometer efficiency. The column depth and pressure broadening (≈10 MHz/Torr) of the atmosphere drop dramatically from the ground to the altitude of balloon float. In broad photometric bands, the upper atmospheric emission is similar to one bounce from a mirror or transmission through a window at ambient temperature. The diminished pressure broadening also opens windows that are much darker than the broadband average, and which become accessible to a spectrometer with resolving power $R > 100$. Observations in these windows also benefit from cryogenic optics. Over 420–540 GHz with $R = 512$, 50% of the channels are 25 times darker than an ambient-temperature optic.

follows: 1) to make a definitive detection of redshifted [CII] [4, 5] (1900-GHz rest frame) in correlation with quasars at redshifts $2.5 < z < 3.5$; 2) to detect two adjacent ladder lines of CO in each of the BOSS samples (MAIN, LOWZ, CMASS); and 3) to constrain both CO $J = 4 - 3$ and [CI] (492 GHz) in the Milky Way. Current models of the diffuse, redshifted CO and [CII] intensity vary by nearly two orders of magnitude [6, 7, 8, 9, 10]. EXCLAIM's IM measurements of two J lines at the same redshift will permit new diagnostics of the ISM environment. Additionally, EXCLAIM's measurements of the integrated emission will complement interferometric observations by the Atacama Large Millimeter/submillimeter Array (ALMA) [11]. In the Milky Way, [CI] emission can track molecular gas in regions where CO is photodissociated. Thus, EXCLAIM will provide insight into the relation between CO and molecular gas.

EXCLAIM will use an all-cryogenic (< 4 K) telescope that provides the high sensitivity (see Fig. 1 for the expected photon loading) required to achieve these goals in a one-day conventional balloon flight from North America (Texas or New Mexico). This type of flight provides excellent access to the BOSS regions besides offering easy logistics and reuse possibilities. The combination of a cold telescope with a moderate-resolution spectrometer and with observations from a stratospheric balloon will allow EXCLAIM to observe with sufficient sensitivity in the dark regions between atmospheric lines that are broadened into a continuum at lower altitudes.

The EXCLAIM program began in April 2019 and is approaching the end of its preliminary design and technology completion stage, with several systems already in their final design phase. An engineering flight to test all the systems with one spectrometer is planned in 2022. Following refurbishment, science flights with six spectrometers will start as early as 2023. This manuscript will guide the reader through every major system and will conclude presenting detection forecasts.

2. Cryogenic telescope

Following Fig. 2, the infrared radiation enters the telescope at an elevation angle of 45° and is reflected off of a 90-cm (74-cm projected) monolithic aluminum parabolic primary mirror [12, 13] to a secondary and tertiary mirror. The projected aperture size provides a resolution of $4'$ full width at half maximum (FWHM), permitting a survey that covers spatial scales from the linear regime, $k \lesssim 0.1h/\mathrm{Mpc}$, up to scales where shot noise dominates, $k \gtrsim 5h/\mathrm{Mpc}$ [14]. The mirrors couple the light to the cryogenic (1.7 K) receiver, which houses the focal plane with one or more spectrometers operating at $\lesssim 125$ mK.

The EXCLAIM telescope and receiver will be housed in a liquid-helium Dewar, with an inner diameter of 152 cm and identical in design to the Absolute Radiometer for

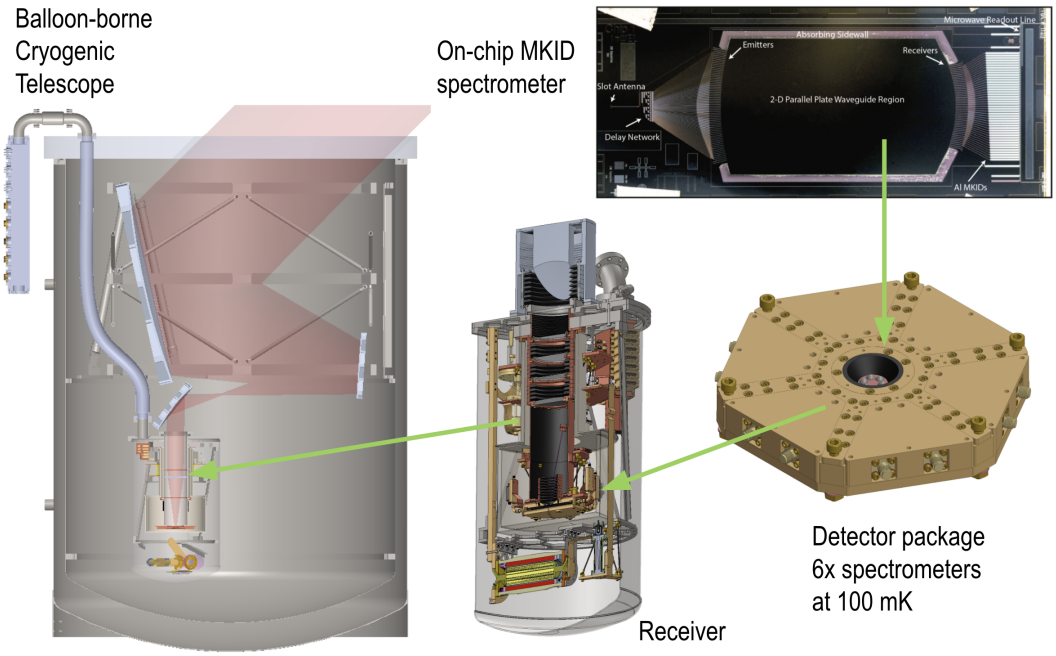

Fig. 2: EXCLAIM employs a cryogenic telescope to reach high sensitivity in spectral windows of low emission in the upper atmosphere. The telescope and receiver are located in a bucket dewar capable of 3500 liters of liquid-helium to provide 24 hours of 1.7-K operations at float altitude. The receiver houses the focal plane with six spectrometers operating at $\lesssim$ 125 mK, as well as the amplifiers and sub-kelvin cooler.

Cosmology, Astrophysics, and Diffuse Emission II (ARCADE II) [15] and the Primordial Inflation Polarization ExploreR (PIPER) [13] instruments. An initial fill of 3500 liters will provide 24 hours of 1.7-K operation at a float altitude greater than 27 km. A swiveling lid will insulate the instrument on the ground and in ascent. At float altitude, positive pressure from boil-off gas will act to keep the cryogenic optics dry and clean, eliminating the need for windows at ambient temperature. ARCADE II and PIPER have similar open aperture areas and have demonstrated positive pressure and clean optics. A 2017 PIPER engineering flight [16] showed that superfluid fountain-effect pumps could maintain large telescope optical elements at 1.7 K.

3. Receiver

The receiver houses the spectrometers, amplifiers and sub-Kelvin cooler, and will remain superfluid-tight. EXCLAIM's window into the receiver will be either anti-reflective (AR)-coated [17] quartz (for which PIPER has demonstrated a superfluid indium seal that accommodates the coefficient of thermal expansion and does not rupture on parachute or landing shock) or AR-coated silicon. The receiver optics will couple the reflective telescope to AR-coated silicon hyper-hemispherical lenslets placed over the on-chip spectrometer slot antennas [18, 19]. Cryogenic housekeeping harnesses and the spectrometer readout will route to ambient-temperature electronics via thin-wall stainless-steel bellows.

A single-shot Adiabatic Demagnetization Refrigerator (ADR) [20, 21] will provide a 100-mK base temperature and 1 μW of cooling power for the spectrometer focal plane. Niobium-titanium (NbTi) coaxial cables [22] and carbon fiber suspensions will be employed to isolate the 100-mK stage from a 900-mK intermediate stage. The intermediate stage is cooled by a ^{4}He cooler. The high-current ADR magnet leads will be vapor-cooled and enter the receiver through a superfluid-tight feedthrough.

4. Integrated spectrometer

The focal plane of the EXCLAIM instrument will feature six μ-Spec [23, 24, 25] spectrometers. μ-Spec is a diffraction-grating analog spectrometer, which integrates all of its components, including the detectors, onto a compact silicon (Si) chip. A slot-antenna couples to planar niobium (Nb) transmission lines and the diffraction grating is synthesized in a microstrip line delay network. This network introduces a linear phase gradient and then launches the signals into a Nb 2D parallel-plate waveguide region via an array of emitting and receiving feeds that are arranged in a Rowland configuration [26, 27]. These receivers Nyquist-sample the spectrometer's spec-

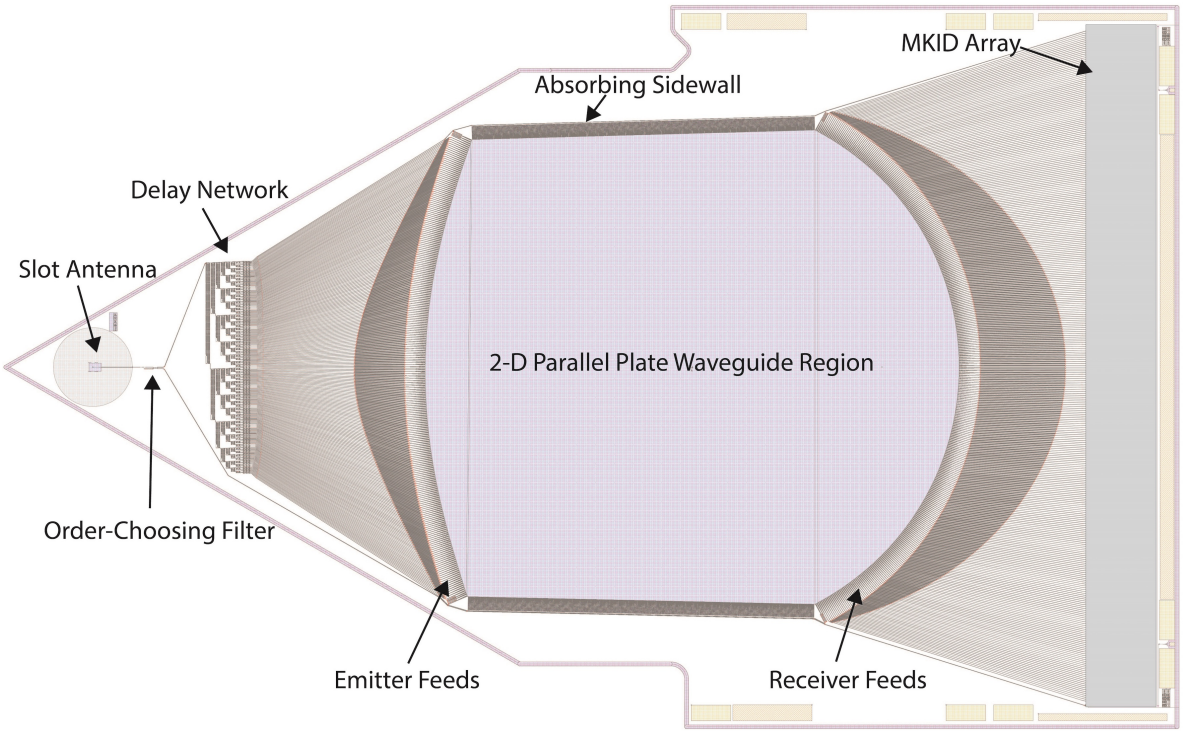

Fig. 3: The EXCLAIM spectrometer design.

tral function, which is close to a sinc^2 function, the Fourier transform of a uniformly illuminated synthetic grating. Each received signal is then transmitted to individual microwave kinetic inductance detectors (MKIDs).

Fig. 3 shows the EXCLAIM μ-Spec design. Each spectrometer will provide a resolving power $R = 512$ over the 420–540 GHz spectral band. The spectrometer is designed [28] to operate over a single grating order, $M = 2$, which is selected by a combination of: 1) metal mesh filters inserted in the receiver optics tube; 2) an on-chip order-choosing filter; and 3) the Nb transmission lines, which block transmission above the superconducting gap frequency of approximately 680 GHz. The microstrip line architecture of the spectrometer, which employs a protective Nb ground plane layer under a thin 450-nm-thick Si dielectric layer, also provides high immunity to stray light and cross-talk. In addition, a thin-film titanium (Ti) coating will be deposited on the back of the spectrometer chip to terminate stray light. The option of placing thermal blocking filters [29, 30] on the microwave input and output lines is currently under consideration.

Each EXCLAIM spectrometer will feature 355 half-wave aluminum-niobium (Al-Nb) microstrip transmission line MKIDs, with 20-nm-thick Al, operating at near background-limited sensitivity and read out on a single microwave readout line. These thin Al films, which serve as the absorbing layer in the EXCLAIM MKID design, have demonstrated internal quality factors Q_{int} of $(1\text{–}4) \times 10^6$, and long quasi-particle lifetimes of approximately 1 ms, when measured in coplanar-waveguide resonators [31]. Likewise, Nb films have been demonstrated in coplanar-waveguide resonators with Q_{int} of $(5\text{–}8) \times 10^5$ [32].

The fabrication of the spectrometer circuitry on the single-crystal Si dielectric is done using a wafer-scale bonding technique [33]. A Nb liftoff patterning process is used, which provides precision control of line width [33] to ensure the necessary phase control in the spectrometer transmission lines and avoids damaging the thin Si dielectric substrate. Single-crystal Si is chosen due to its low-loss [34, 35], which enables near-unity efficiency and resolutions [36, 25] up to $R = 1500$ in principle. In practice, the EXCLAIM spectrometer efficiency is expected to be limited not by transmission-line loss, but by the individual efficiencies of the sub-millimeter component designs, with a total expected spectrometer efficiency conservatively assumed to be around 30%.

5. Instrument electronics and flight software

The EXCLAIM detector readout electronics baseline design includes a Xilinx ZCU111 Radio Frequency System-on-Chip (RFSoC). An ongoing trade study shows clear advantages in terms of performance, mass and power

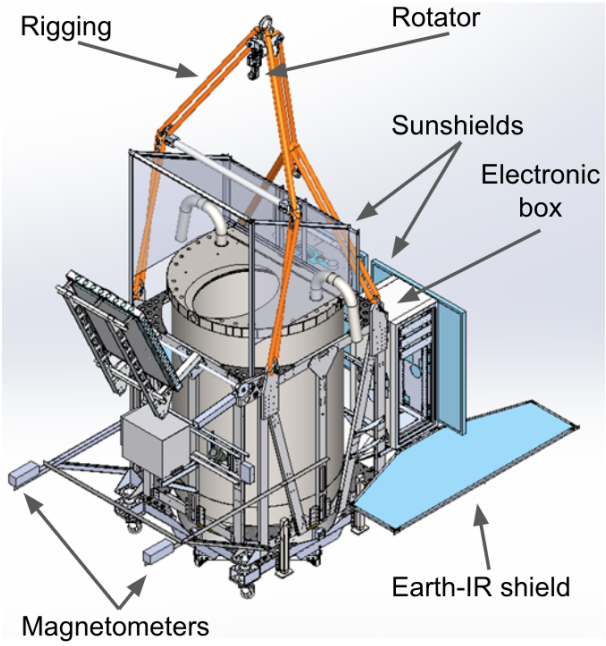

Fig. 4: The complete payload. A rotator pivot connects EXCLAIM to the flight train of the balloon through a rigging that holds the entire payload. The different shields will enable passive thermal control. The magnetometers will serve as attitude determination sensors along with a star camera, gyroscopes, sun sensors and clinometers (not shown).

over a Reconfigurable Open Architecture Computing Hardware 2 (ROACH-2) system [37], which was extensively used in previous balloon missions such as The Next Generation Balloon-borne Large Aperture Submillimeter Telescope (BLAST-TNG) [38] and the Far Infrared Observatory Mounted on a Pointed Balloon (OLIMPO) [39]. Intermediate frequency hardware will mix the digital-to-analog converter (DAC) output from either a RFSoC or ROACH-2 to ≈3.5-GHz MKID resonance frequency range and will mix the spectrometer output down for input to the analog-to-digital converter (ADC). The readout provides 512-MHz radio frequency (RF) bandwidth, and will read the spectrometer array at 488 Hz.

The electronics for the ADR, cryogenic and gondola housekeeping, attitude determination and control, power control and telemetry interface will be based on PIPER, although with a number of variations dictated by the different requirements and constraints. The flight software and low-power flight computers will also follow the PIPER design approach, demonstrated in the PIPER 2017 engineering flight.

6. Thermal control

Except for the receiver, the thermal control of the instrument will be done primarily passively, although localized heaters will be used as needed. The flight electronics (Fig. 4) will be stored in a 33U rack, while the detector readout electronics in a 14U rack.[1] Both are standard 19-inch-wide racks. The batteries will be located underneath the 14U rack to ensure the payload is balanced. To maintain the electronics temperature between $-40°$C and $+20°$C, thermal control will be guaranteed by one or more radiators, as well as white paints to eliminate excess heat. Foam panels and heaters will be used to keep the electronics warm during ascent when then temperatures can drop below $-50°$C.

Additional multilayer insulation (MLI) radiation shields will be placed around the payload (Fig. 4) to reduce the amount of solar and Earth infrared radiation. An additional sunshield will be added above the lid to reduce solar radiation on the telescope aperture during daytime operations.

7. Observing strategy

EXCLAIM will scan in azimuth at constant elevation and map a strip across a constant range of declination. Unlike the auto-power [40], a cross-power detection does not suffer a penalty toward large survey areas. Thus, EXCLAIM seeks to maximize the survey area to access linear modes while also sampling the beam in the scan and sky drift directions. For a flight from Ft. Sumner, New Mexico, the provisional survey region encompasses Sloan Stripe 82. Primary science observations will occur when the sun is down, but additional regions may be achievable in an anti-solar scan pattern during the day.

EXCLAIM has modest pointing requirements to conduct a large-area survey within the BOSS regions. In flight, a reaction wheel will scan the payload about a central azimuth to enable the primary scanning strategy. A rotator pivot to the flight train provides torque to desaturate the reaction wheel by dumping momentum to the balloon. The reaction wheel and rotator are sized to provide control torque at least equal to worst-case disturbances. A magnetometer and a star camera will determine an instantaneous reference to the scan center azimuth. Sun sensors will be used primarily in sun avoidance during the day time, but possibly also as a cross-check on the magnetometer for absolute pointing determined in-line. Post-flight pointing reconstruction will use data from an array of gyroscopes, accelerometers, tilt sensors and the magnetometer to tie together star camera determinations, which will provide ≈ 3” pointing at 1-Hz intervals.

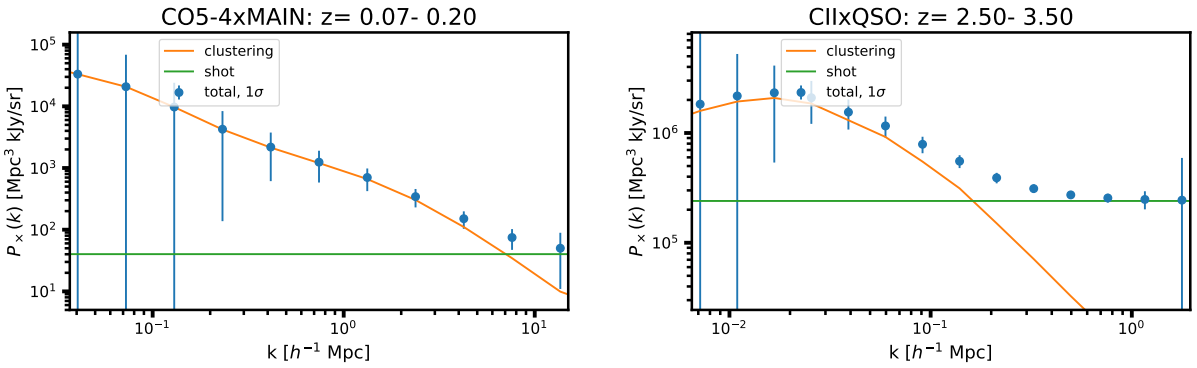

Fig. 5: Forecast for cross-correlations of CO $J = 5 - 4 \times$ SDSS MAIN at $0.07 < z < 0.2$ (left) and [CII] $\times$ BOSS QSO at $2.5 < z < 3.5$ (right) assuming signal levels from Refs. [6, 4], respectively. The low redshift correlations trace nonlinear scales and are expected to have limited correlated shot noise. The high-redshift [CII] probes linear scales and is expected to have a higher level of correlated shot noise.

8. Anticipated sensitivity

The sensitivity for intensity mapping is estimated using both a numerically simple mode counting argument for the three-dimensional power spectrum [7, 41, 42] and using a simulated analysis of angular cross-correlations between redshift slices [43]. Both estimates agree and include the effects of angular and spectral resolution and survey volume. The three-dimensional power spectrum approach requires homogeneous noise in the frequency direction, and an inverse-noise weighted effective noise is used for the volume, which is validated by simulations. Shot noise in the galaxy sample is given by published values of $\bar{n}$ [3, 44].

The specification of the detector performance must take several factors into account: 1) MKID noise contributions are loading-dependent, 2) the power absorbed by the MKID depends on the efficiency of the complete spectrometer system, and 3) MKIDs generically have $1/f$ noise contributions from two-level systems [45]. To accommodate these factors, the sensitivity of the spectrometer is specified under expected optical loading as a multiplier of the photon background-limit (including optically-excited quasiparticle fluctuations), referring to the power incident at the spectrometer lenslet, and weighted over acoustic frequencies of the science signal (5–25 Hz, unless additional modulation is employed). The spectrometer NEP for these baseline forecasts is taken to be a factor of three over the background limit, though considerably poorer NEP performance will still accomplish the EXCLAIM mission threshold detection goals. As shown in Fig. 5, the expected 2σ sensitivity to the surface brightness-bias product for $0 < z < 0.2$ (SDSS MAIN) for CO $J = 4 - 3$, $J = 5 - 4$, $0.2 < z < 0.4$ for $J = 5 - 4$, $J = 6 - 5$ (BOSS LOWZ), $0.4 < z < 0.7$ for $J = 6 - 5$ (CMASS), and $2.5 < z < 3.5$ for [CII] (QSO) are $\{0.15, 0.28, 0.30, 0.37, 0.45, 13\}$ kJy/sr, respectively.

[1]A rack unit, or "U", is a unit of measure defined as 1.75 inches (44.45 mm). It is used as a measurement of the overall height of 19- and 23-inch-wide rack frames.

Acknowledgments

Funding provided by the NASA Astrophysics Research and Analysis (APRA) program is gratefully acknowledged, as well as funding from the Space Grant in support of many of the EXCLAIM interns.

References

[1] P. Madau and M. Dickinson. Cosmic Star-Formation History. *Annu. Rev. Astron. Astrophys.*, 52:415–486, 2014.

[2] C. L. Carilli and F. Walter. Cool Gas in High-Redshift Galaxies. *Annu. Rev. Astron. Astrophys.*, 51:105–161, 2013.

[3] B. Reid, S. Ho, N. Padmanabhan, W.J. Percival, J. Tinker, R. Tojeiro, M. White, D.J. Eisenstein, C. Maraston, A.J. Ross, A.G. Sánchez, D. Schlegel, E. Sheldon, M.A. Strauss, D. Thomas, D. Wake, F. Beutler, D. Bizyaev, A. S. Bolton, J.R. Brownstein, C.-H. Chuang, K. Dawson, P. Harding, F.-S. Kitaura, A. Leauthaud, K. Masters, C.K. McBride, S. More, M.D. Olmstead, D. Oravetz, S. E. Nuza, K. Pan, J. Parejko, J. Pforr, F. Prada, S. Rodríguez-Torres, S. Salazar-Albornoz, L. Samushia, D.P. Schneider, C. G. Scóccola, A. Simmons, and M. Vargas-Magana. SDSS-III Baryon Oscillation Spectroscopic Survey Data Release 12: galaxy target selection and large-scale structure catalogues. *Mon. Not. R. Astron. Soc*, 455:1553–1573, 2016.

[4] S. Yang, A.R. Pullen, and E.R. Switzer. Evidence for C II diffuse line emission at redshift $z \sim 2.6$. *Mon. Not. R. Astron. Soc*, 489(1):L53–L57, 2019.

[5] H. Padmanabhan. Constraining the evolution of [C II] intensity through the end stages of reionization. *Mon. Not. R. Astron. Soc*, 488(3):3014–3023, 2019.

[6] A.R. Pullen, T.-C. Chang, O. Doré, and A. Lidz. Cross-correlations as a Cosmological Carbon Monoxide Detector. *Astrophys. J.*, 768:15, 2013.

[7] A. Lidz, S.R. Furlanetto, S.P. Oh, J. Aguirre, T.-C. Chang, O. Doré, and J.R. Pritchard. Intensity Mapping with Carbon Monoxide Emission Lines and the Redshifted 21 cm Line. *Astrophys. J.*, 741:70, 2011.

[8] M. Righi, C. Hernández-Monteagudo, and R.A. Sunyaev. Carbon monoxide line emission as a CMB foreground: tomography of the star-forming universe with different spectral resolutions. *Astron. Astrophys.*, 489:489–504, 2008.

[9] E. Visbal and A. Loeb. Measuring the 3D clustering of undetected galaxies through cross correlation of their cumulative flux fluctuations from multiple spectral lines. *J. Cosmol. Astropart. Phys.*, 11:16, 2010.

[10] G. Popping, E. van Kampen, R. Decarli, M. Spaans, R.S. Somerville, and S.C. Trager. Sub-mm emission line deep fields: CO and [C II] luminosity functions out to z = 6. *Mon. Not. R. Astron. Soc.*, 461:93–110, 2016.

[11] R. Decarli, F. Walter, J. Gónzalez-López, M. Aravena, L. Boogaard, C. Carilli, P. Cox, E. Daddi, G. Popping, D. Riechers, B. Uzgil, A. Weiss, R.J. Assef, R. Bacon, F.E. Bauer, F. Bertoldi, R. Bouwens, T. Contini, P.C. Cortes, E. da Cunha, T. Díaz-Santos, D. Elbaz, H. Inami, J. Hodge, R. Ivison, O. Le Fèvre, B. Magnelli, M. Novak, P. Oesch, H.-W. Rix, M.T. Sargent, I.R. Smail, A.M. Swinbank, R.S. Somerville, P. van der Werf, J. Wagg, and L. Wisotzki. The ALMA Spectroscopic Survey in the HUDF: CO luminosity functions and the molecular gas content of galaxies through cosmic history. *Astrophys. J.*, 882(2):138, 2019.

[12] K. Harrington, T. Marriage, A. Ali, J.W. Appel, C.L. Bennett, F. Boone, M. Brewer, M. Chan, D.T. Chuss, F. Colazo, S. Dahal, K. Denis, R. Dünner, J. Eimer, T. Essinger-Hileman, P. Fluxa, M. Halpern, G. Hilton, G.F. Hinshaw, J. Hubmayr, J. Iuliano, J. Karakla, J. McMahon, N.T. Miller, S. H. Moseley, G. Palma, L. Parker, M. Petroff, B. Pradenas, K. Rostem, M. Sagliocca, D. Valle, D. Watts, E. Wollack, Z. Xu, and L. Zeng. The Cosmology Large Angular Scale Surveyor. In *Millimeter, Submillimeter, and Far-Infrared Detectors and Instrumentation for Astronomy VIII*, volume 9914 of *Proc. SPIE*, page 99141K, 2016.

[13] N.N. Gandilo, P.A.R. Ade, D. Benford, C.L. Bennett, D.T. Chuss, J.L. Dotson, J.R. Eimer, D.J. Fixsen, M. Halpern, G. Hilton, G.F. Hinshaw, K. Irwin, C. Jhabvala, M. Kimball, A. Kogut, L. Lowe, J.J. McMahon, T.M. Miller, P. Mirel, S.H. Moseley, S. Pawlyk, S. Rodriguez, E. Sharp, P. Shirron, J.G. Staguhn, D.F. Sullivan, E.R. Switzer, P. Taraschi, C.E. Tucker, and E.J. Wollack. The Primordial Inflation Polarization Explorer (PIPER). In *Millimeter, Submillimeter, and Far-Infrared Detectors and Instrumentation for Astronomy VIII*, volume 9914 of *Proc. SPIE*, page 99141J, 2016.

[14] J.L. Bernal, P.C. Breysse, H. Gil-Marín, and E.D. Kovetz. User's Guide to Extracting Cosmological Information from Line-Intensity Maps. *Phys. Rev. D*, 100:123522, 2019.

[15] J. Singal, D.J. Fixsen, A.J. Kogut, S. Levin, M. Limon, P. Lubin, P. Mirel, M. Seiffert, T. Villela, E. Wollack, and C.A. Wuensche. The ARCADE 2 Instrument. *Astrophys. J.*, 730:138, 2011.

[16] S. Pawlyk, P.A.R. Ade, D. Benford, C.L. Bennett, D.T. Chuss, R. Datta, J.L. Dotson, J.R. Eimer, D.J. Fixsen, N.N. Gandilo, T.M. Essinger-Hileman, M. Halpern, G. Hilton, G.F. Hinshaw, K. Irwin, C. Jhabvala, M. Kimball, A. Kogut, L. Lowe, J.J. McMahon, T.M. Miller, P. Mirel, S.H. Moseley, S. Rodriguez, E. Sharp, P. Shirron, J.G. Staguhn, D.F. Sullivan, E.R. Switzer, P. Taraschi, C.E. Tucker, A. Walts, and E.J. Wollack. The primordial inflation polarization explorer (PIPER): current status and performance of the first flight. In *Millimeter, Submillimeter, and Far-Infrared Detectors and Instrumentation for Astronomy IX*, volume 10708 of *Proc. SPIE*, page 1070806, 2018.

[17] D. Koller, A.R. Kerr, G.A. Ediss, and D. Boyd. Design and fabrication of quartz vacuum windows with matching layers for millimeter-wave receivers. *ALMA memo 377*, 2001.

[18] D.F. Filipovic, S.S. Gearhart, and G.M. Rebeiz. Double-slot antennas on extended hemispherical and elliptical silicon dielectric lenses. *IEEE Trans. Microw. Theory Tech.*, 41:1738–1749, 1993.

[19] M. Ji, C. Musante, S. Yngvesson, A. J. Gatesman, and J. Waldman. Study of Parylene as Anti-reflection

Coating for Silicon Optics at THz Frequencies. In *11th Int. Symp. Space THz Technol.*, page 407, 2000.

[20] P.J. Shirron, M.O. Kimball, B.L. James, T.T. Muench, E.R. Canavan, M.J. DiPirro, T.A. Bialas, G.A. Sneiderman, K.R. Boyce, C.A. Kilbourne, F.S. Porter, R. Fujimoto, Y. Takei, S. Yoshida, and K. Mitsuda. Design and on-orbit operation of the soft x-ray spectrometer adiabatic demagnetization refrigerator on the Hitomi observatory. *J. Astron. Telesc. Instrum. Syst.*, 4(2):1–8, 2018.

[21] E.R. Switzer, P.A.R. Ade, T. Baildon, D. Benford, C.L. Bennett, D.T. Chuss, R. Datta, J.R. Eimer, D.J. Fixsen, N.N. Gandilo, T.M. Essinger-Hileman, M. Halpern, G. Hilton, K. Irwin, C. Jhabvala, M. Kimball, A. Kogut, J. Lazear, L.N. Lowe, J.J. McMahon, T.M. Miller, P. Mirel, S.H. Moseley, S. Pawlyk, S. Rodriguez, E. Sharp, P. Shirron, J.G. Staguhn, D.F. Sullivan, P. Taraschi, C.E. Tucker, A. Walts, and E.J. Wollack. Sub-Kelvin cooling for two kilopixel bolometer arrays in the PIPER receiver. *Rev. Sci. Instrum.*, 90(9):095104, Sep 2019.

[22] A.B. Walter, C. Bockstiegel, B.A. Mazin, and M. Daal. Laminated NbTi-on-Kapton Microstrip Cables for Flexible Sub-Kelvin RF Electronics. *IEEE Trans. Appl. Supercond.*, 28:2500105, 2017.

[23] G. Cataldo, W.-T. Hsieh, W.-C. Huang, S.H. Moseley, T.R. Stevenson, and E.J. Wollack. Micro-Spec: an ultracompact, high-sensitivity spectrometer for far-infrared and submillimeter astronomy. *Appl. Opt.*, 53:1094, 2014.

[24] G. Cataldo, S.H. Moseley, and E.J. Wollack. A four-pole power-combiner design for far-infrared and submillimeter spectroscopy. *Acta Astronaut.*, 114:54–59, 2015.

[25] E.M. Barrentine, G. Cataldo, A.-D. Brown, N. Ehsan, O. Noroozian, T.R. Stevenson, K. U-Yen, E.J. Wollack, and S.H. Moseley. Design and performance of a high resolution μ-Spec: an integrated sub-millimeter spectrometer. In *Millimeter, Submillimeter, and Far-Infrared Detectors and Instrumentation for Astronomy VIII*, volume 9914 of *Proc. SPIE*, page 99143O, 2016.

[26] H.A. Rowland. On concave gratings for optical purposes. *Philos. Mag.*, 16:197–210, 1883.

[27] W. Rotman and R. Turner. Wide-angle microwave lens for line source applications. *IEEE Trans. Antennas Propag.*, 11(6):623–632, 1963.

[28] G. Cataldo, E.M. Barrentine, B.T. Bulcha, N. Ehsan, L.A. Hess, O. Noroozian, T.R. Stevenson, E.J. Wollack, S.H. Moseley, and E.R. Switzer. Second-generation Micro-Spec: A compact spectrometer for far-infrared and submillimeter space missions. *Acta Astronaut.*, 162:155–159, 2019.

[29] K. U-Yen and E.J. Wollack. Compact planar microwave blocking filter. In *Microwave Conference, 2008. EuMC 2008. 38th European*, pages 642–645, 2008.

[30] E.J. Wollack, D.T. Chuss, K. Rostem, and K. U-Yen. Impedance matched absorptive thermal blocking filters. *Rev. Sci. Instrum.*, 85(3):034702, 2014.

[31] O. Noroozian, E.M. Barrentine, T.R. Stevenson, A.-D. Brown, V. Mikula, K. U-Yen, E.J. Wollack, and S.H. Moseley. Photon Counting Kinetic Inductance Detectors for THz/Submillimeter Space Spectroscopy. In *17th International Workshop on Low Temperature Detectors*, 2017.

[32] L. A. Hess, E. M. Barrentine, A. D. Brown, A. Gangopadhyay, K. Livi, M. Mirzaei, S. H. Moseley, O. Noroozian, T. R. Stevenson, and E. R. Switzer. Low-Loss Microstrip Transmission Line Fabricated with Improved Liftoff Process. In *18th International Workshop on Low Temperature Detectors*, 2019.

[33] A. Patel, A.-D. Brown, W.-T. Hsieh, T.R. Stevenson, S.H. Moseley, K. U-Yen, N. Ehsan, E.M. Barrentine, G. Manos, and E.J. Wollack. Fabrication of MKIDS for the Micro-Spec Spectrometer. *IEEE Trans. Appl. Supercond.*, 23(3):2400404, 2013.

[34] M. N. Afsar and H. Chi. Millimeter wave complex refractive index, complex dielectric permittivity and loss tangent of extra high purity and compensated silicon. *J. Infrared Millim. Terahertz Waves*, 15:1181–1188, 1994.

[35] E.J Wollack, G. Cataldo, K.H. Miller, and M.A. Quijada. Infrared properties of high-purity silicon. *Opt. Lett.*, 45(17):4935–4938, 2020.

[36] G. Cataldo, E.M. Barrentine, B.T. Bulcha, N. Ehsan, L.A. Hess, O. Noroozian, T.R. Stevenson, K. U-Yen, E.J. Wollack, and S.H. Moseley. Second-generation design of Micro-Spec: a medium-resolution, submillimeter- wavelength spectrometer-on-a-chip. *J. Low Temp. Phys.*, 193:923–930, 2018.

[37] J. Hickish, Z. Abdurashidova, Z. Ali, K.D. Buch, S.C. Chaudhari, H. Chen, M. Dexter, R.S. Domagalski, J. Ford, G. Foster, D. George, J. Greenberg, L. Greenhill, A. Isaacson, H. Jiang, G. Jones,

F. Kapp, H. Kriel, R. Lacasse, A. Lutomirski, D. MacMahon, J. Manley, A. Martens, R. McCullough, M.V. Muley, W. New, A. Parsons, D. C. Price, R. A. Primiani, J. Ray, A. Siemion, V. van Tonder, L. Vertatschitsch, M. Wagner, J. Weintroub, and D. Werthimer. A Decade of Developing Radio-Astronomy Instrumentation using CASPER Open-Source Technology. *J. Astron. Instrum.*, 5:1641001–12, 2016.

[38] N.P. Lourie, P.A.R. Ade, F.E. Angile, P.C. Ashton, J.E. Austermann, M.J. Devlin, B. Dober, N. Galitzki, J. Gao, and S. Gordon. Preflight characterization of the BLAST-TNG receiver and detector arrays. In *Millimeter, Submillimeter, and Far-Infrared Detectors and Instrumentation for Astronomy IX*, volume 10708 of *Proc. SPIE*, pages 52–66, 2018.

[39] A. Paiella, A. Coppolecchia, L. Lamagna, P. A. R. Ade, E. S. Battistelli, M. G. Castellano, I. Colantoni, F. Columbro, G. D'Alessandro, P. de Bernardis, S. Gordon, S. Masi, P. Mauskopf, G. Pettinari, F. Piacentini, G. Pisano, G. Presta, and C. Tucker. Kinetic inductance detectors for the OLIMPO experiment: design and pre-flight characterization. *J. Cosmol. Astropart. Phys.*, 1:039, 2019.

[40] L. Knox. Determination of inflationary observables by cosmic microwave background anisotropy experiments. *Phys. Rev. D*, 52(8):4307–4318, 1995.

[41] A.R. Pullen, O. Doré, and J. Bock. Intensity Mapping across Cosmic Times with the Lyα Line. *Astrophys. J.*, 786:111, 2014.

[42] T.Y. Li, R.H. Wechsler, K. Devaraj, and S.E. Church. Connecting CO Intensity Mapping to Molecular Gas and Star Formation in the Epoch of Galaxy Assembly. *Astrophys. J.*, 817:169, 2016.

[43] A. Loureiro, B. Moraes, F.B. Abdalla, A. Cuceu, M. McLeod, L. Whiteway, S.T. Balan, A. Benoit-Lévy, O. Lahav, M. Manera, R.P. Rollins, and H.S. Xavier. Cosmological measurements from angular power spectra analysis of BOSS DR12 tomography. *Mon. Not. R. Astron. Soc.*, 485:326–355, 2019.

[44] S. Eftekharzadeh, A.D. Myers, M. White, D.H. Weinberg, D.P. Schneider, Y. Shen, A. Font-Ribera, N.P. Ross, I. Paris, and A. Streblyanska. Clustering of intermediate redshift quasars using the final SDSS III-BOSS sample. *Mon. Not. R. Astron. Soc.*, 453(3):2779–2798, 2015.

[45] J. Gao, M. Daal, J.M. Martinis, A. Vayonakis, J. Zmuidzinas, B. Sadoulet, B.A. Mazin, P.K. Day, and H.G. Leduc. A semiempirical model for two-level system noise in superconducting microresonators. *Appl. Phys. Lett.*, 92(21):212504, 2008.